Hindawi
International Journal of Antennas and Propagation
Volume 2022, Article ID 1462193, 8 pages
https://doi.org/10.1155/2022/1462193

Research Article

Design of a Novel Integral Sliding Mode-Based Composite Nonlinear Feedback Controller for Electrostatic MEMS Micromirror

Jun Wu,[1] **Wenbo Zhu**,[1] **Bingjie Guan**,[2] **and Hui Chen**[3]

[1]*School of Mechatronic Engineering and Automation, Foshan University, Foshan, China*
[2]*School of Artificial Intelligence, Henan University, Kaifeng, China*
[3]*College of Eletrical Engineering and Automation, Shandong University of Science and Technology, Qingdao, China*

Correspondence should be addressed to Hui Chen; chenhuijob@126.com

Received 15 December 2021; Accepted 4 March 2022; Published 31 March 2022

Academic Editor: Bin Zhang

In this study, the precise tracking problem for electrostatic micromirror systems with disturbances and input saturation is investigated. Inspired by the composite nonlinear feedback (CNF)'s improvement of the transient performance and the sliding mode control's enhancement of the robustness, a novel integral sliding mode with reaching law (ISMRL)-based composite nonlinear feedback (CNF) controller is proposed. Then, the stability of the closed-loop system is proved based on Lyapunov theorem. Finally, numerical simulations are investigated to evaluate the effectiveness of the proposed scheme. It is shown that the closed-loop system with the proposed scheme has precise positioning and improved transient performance in presence of time-varying disturbances.

1. Introduction

Micro-electro-mechanical system (MEMS) micromirror has experienced enormous commercial success in applications such as optical switches [1, 2], biomedical imaging [3], and high-resolution displays [4]. Compared with electrothermal, electromagnetic, and piezoelectric actuation, the advantages of electrostatic actuation are fast response, simple electronic driving, and low power consumption [5]. However, the electrostatic MEMS micromirror suffers unsatisfied transient performance and pull-in instability under open loop control. Lots of efforts and control strategies have been introduced to tackle the problem. Classic strategies, such as PID controller [6, 7], H-infinity robust controller [8], sliding mode control [9], and adaptive control [10] schemes have been reported to improve its tracking performance and eliminate the effect of external disturbances. The aforementioned control strategies have been verified benefits of improving the positioning performance and extending the stable operational range of micromirrors. However, the transient response, which is essential for micromirror's application, is not directly considered. For instant, fast setting time and low overshoot of micromirror-based optical switches are required in order to reduce the insertion loss.

For the past few years, composite nonlinear feedback (CNF) control scheme has attracted many attentions as its meaningful improvements in transient behaviors [11]. This scheme was first studied for a class of second-order linear system [12]. Then, it was extended to partially linear composite system [13]. CNF control methods are also investigated for master/slave synchronization of nonlinear system [14], nonlinear time-delay systems [15], strict-feedback nonlinear systems [16], and under actuated systems [17]. The output tracking problem of time-varying references in descriptor systems is investigated using CNF control technique in [18]. Besides developments in theory, the CNF controller is proposed for hard-disk-drive (HDD) servo system [19], spacecraft rendezvous systems [20], multiquadrotor systems [21], robot manipulators [22], and autonomous vehicles [23]. However, when considering the inevitable external disturbances, the traditional CNF control reveals its lack of the ability to deal with it. Fortunately, in the field of control theory, sliding mode control is considered to be a solution for alleviating the effects of the parametric uncertainties and external disturbances [24–26]. As a result, the sliding mode control techniques combined with composite nonlinear feedback are proposed to improve system robustness in [27–38]. Recently, this scheme is also developed for more general class of linear and nonlinear systems with plant uncertainties [39].

Though sliding mode-based CNF controller has been fully studied and demonstrated the advantages of robustness, the chattering problem of sliding mode control is a serious situation which not only increases energy consumption but also leads to the instability. To avoid this, one solution is to introduce the second-order sliding mode control [40]. In [41], a super-twisting algorithm-based integral sliding mode control with composite nonlinear feedback control is proposed to eliminate the chattering effect for magnetic levitation system. Another effective solution to reduce the chattering is the sliding mode control based on the reaching law, which is first proposed in [42]. Recently, in [43–45], improved quick reaching law is proposed to speed up the response and reduce the chattering of a sliding mode control system simultaneously.

Motivated by the aforementioned problem through literature review, the main contribution of this research is that a novel integral sliding mode with reaching law-based composite nonlinear feedback (ISMRL-CNF) controller for angular control of an electrostatic MEMS micromiror is proposed. The CNF controller is designed to guarantee the system has fast dynamic performance and small overshoot. An integral sliding mode control with quick reaching law is designed to enhance the robustness, attenuate chattering, and achieve finite-time convergence of the sliding mode. Furthermore, the time-varying disturbances and input saturation are taken into account for controller design and stability analysis. Simulation study verifies that the closed-loop system with the proposed scheme has precise positioning and improved transient performance in presence of time-varying disturbances.

The rest of the paper is organized as follows. The dynamic model is described in Section 2. The design procedure of the proposed controller and stability analysis are developed in Section 3. Simulation study is given in Section 4. Finally, the conclusions are discussed.

2. The Simplified Dynamics of Electrostatic MEMS Micromirror

Figure 1 shows the schematic figure of a 2-degree-of-freedom electrostatic torsional MEMS micromirror. The studied micromirror consists of mirror plate, torsion bar, gimbal frame, and bottom and sidewall electrodes. The mirror plate is suspended by double frame structure and driven by electrostatic torque. When the driving voltage applied to the bottom and sidewall electrodes, the mirror plate is actuated about X-axis and Y-axis, respectively. The dynamic equations of the system are given as follows [5]:

$$\begin{aligned} (J_1 + J_2)\ddot{\alpha} + D_1\dot{\alpha} + K_1\alpha &= T_\alpha, \\ J_1\ddot{\beta} + D_2\dot{\beta} + K_2\beta &= T_\beta, \end{aligned} \tag{1}$$

where α and β represent the tilt angles of x-axis and y-axis, J_1 and J_2 denote the mass moment of inertias of the mirror plate and gimbal, respectively, D_1 and D_2 represent the damping coefficients, K_1, K_2 represent the stiffness coefficients, and T_α and T_β are electrostatic torque. Introducing the parameter $\tau = \sqrt{K_2/J_1}t$, let $x_1 = \alpha$, $x_2 = d\alpha/d\tau$, $x_3 = \beta$, and $x_4 = d\beta/d\tau$. As a result, system (1) can be described as [5]

$$\begin{aligned} \dot{x}_1 &= x_2, \\ \dot{x}_2 &= -R_1x_2 - \lambda_{\alpha\beta}x_1 + G_1T_\alpha, \\ \dot{x}_3 &= x_4, \\ \dot{x}_4 &= -R_2x_4 - x_3 + G_2T_\beta, \end{aligned} \tag{2}$$

where the parameters are $R_1 = 0.16$, $R_2 = 0.15$, $\lambda_{\alpha\beta} = 0.2251$, $G_1 = 3.0827 \times 10^6$, and $G_2 = 1.7894 \times 10^7$. Considering input saturation and external disturbances, the system is rewritten as

$$\begin{aligned} \dot{x} &= Ax + B\mathrm{sat}(u) + B\ d, \\ y &= Cx, \end{aligned} \tag{3}$$

where $x \in R^n$ is the state of micromirror system, $u \in R$ is the control input, $y \in R$ is the measurement output, And $A, B,$ and C are constant appropriate dimensional matrices. The saturation function $\mathrm{sat}(\cdot)$: $R \longrightarrow R$ is defined as $\mathrm{sat}(u) = \mathrm{sgn}(u)\min\{u_{\max}, |u|\}$ with the maximum of control input $u_{\max}$. The system uncertainties and disturbances $d \in R$ are bounded, and $|d| \le d_{\max}$ with the maximum of disturbances $d_{\max}$. The following assumptions are satisfied for the investigated system (3) [19]: (1) (A, B) is stabilizable, (2) (A, B, C) is invertible, which means the system has no zeros at $s = 0$, and (3) (A, C) is detectable.

3. The Proposed Integral Sliding Mode-Based Composite Nonlinear Feedback Controller Design

In this section, a novel integral sliding mode-based composite nonlinear feedback (ISMRL-CNF) controller is designed for the micromirror system with input saturation and disturbances. The objective is to ensure that the controlled output can track step command input precisely with enhanced transient performance and robustness, in presence of external disturbances. The proposed controller consists of a CNF control law and an integral sliding mode control with reaching law (ISMRL):

$$u = u_N + u_{is}, \tag{4}$$

where the CNF control u_N is utilized to achieve good transient performance and the integral sliding mode control

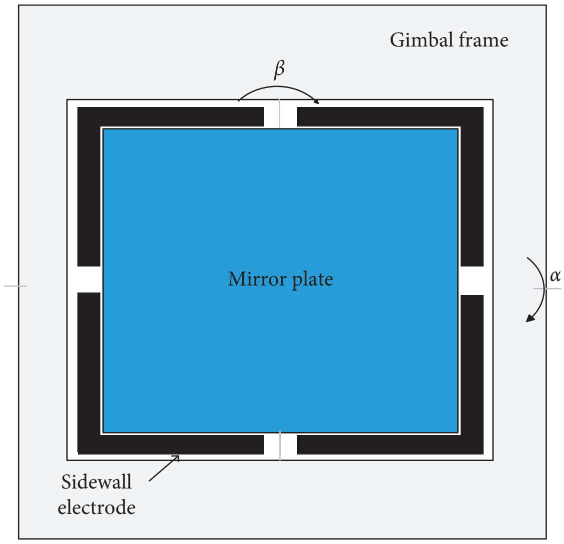

Figure 1: The electrostatic torsional MEMS micromirror.

with reaching law u_{is} is designed to guarantee the system robustness under disturbances and reduce chattering.

The CNF controller consists of a linear control law and a nonlinear control law. The linear control law is presented to achieve fast response by using small damping ration. The nonlinear control law is developed to change the damping ration in order to eliminate overshoot. The linear feedback control u_L is designed as [12]

$$u_L = Fx + Gr, \tag{5}$$

where F is chosen to guarantee that $(A + \mathrm{BF})$ an asymptotically stable matrix, r is a step command input, and G is scalar and calculated as

$$G = -\left[C(A + \mathrm{BF})^{-1}B\right]^{-1}, \tag{6}$$

where F and G are defined since (A, B, C) is assumed to have no invariant zeros at $s = 0$.

The nonlinear feedback law u_{NL} is designed as

$$u_{\mathrm{NL}} = \rho(y, r)B^T P(x - x_e), \tag{7}$$

where $\rho(y, r)$ represents any nonpositive nonlinear function. Different forms of $\rho(y, r)$ have been reported in previous works. A scaled nonlinear function is proposed to adapt the variation of tracking targets in [19] as

$$\rho(y, r) = -\overline{\beta} e^{-m(y-r)}, \tag{8}$$

where $\overline{\beta}$ and m are positive tunable parameters. Define P as a real positive definite symmetric matrix which can be solved from the Lyapunov equation:

$$(A + \mathrm{BF})^T P + P(A + \mathrm{BF}) = -W. \tag{9}$$

With a given positive definite symmetric matrix W, consider that P always exists since $(A + \mathrm{BF})$ is defined to be asymptotically stable. W can be chosen as

$$W = 10^{\theta} \cdot \widehat{E}, \tag{10}$$

where θ is a tunable parameter and $\widehat{E}$ is an identity matrix. Then, the new steady-state value x_e is computed as

$$x_e = -(A + \mathrm{BF})^{-1}\mathrm{BG}r. \tag{11}$$

Finally, a CNF controller is formed by combining the linear feedback law (5) and the nonlinear feedback law (7) as follows:

$$\begin{aligned} u_N &= u_L + u_{\mathrm{NL}} \\ &= Fx + Gr + \rho(y, r)B^T P(x - x_e), \end{aligned} \tag{12}$$

Theorem 1. *For any $\delta \in (0, 1)$, choosing $c_\delta > 0$ to be the largest positive scalar and satisfying the conditions [27],*

$$|Fx| \le (1 - \delta)u_{\max}, \forall x \in X_\delta := \left\{x | x^T P x \le c_\delta\right\}. \tag{13}$$

The initial state x_0 and r satisfy

$$x_0 - x_e \in X_\delta, |Hr| \le \delta_1 u_{\max}, \tag{14}$$

where $H = [I - F(A + BF)^{-1}B]G$, $0 \le \delta_1 < \delta$, and $|(\delta - \delta_1)u_{\max}| = d_{\max}$. Then, the control law (12) is capable to drive the system output y to track the commend input r asymptotically for any nonpositive function $\rho(y, r)$.

Inspired by the robustness enhancement of the integral sliding mode control with reaching law, such a controller is designed and added with the CNF controller to make overall system robust. Taking into account the input saturation, the integral sliding surface is designed as [38]

$$s = B^{+}\left(x(t) - x_0 - \int_o^t Ax(\tau) + B\left(\mathrm{sat}(u) - u_{is}\right)(\tau)d\tau\right), \tag{15}$$

where B^{+} is the pseudoinverse of B and u_{is} is sliding mode control. The reaching law approach is first proposed in [42] which is utilized to force the system state quickly arrives at the sliding mode surface in the whole approaching process [43]. A novel improved quick reaching law is designed as [44]

$$\dot{s} = -k_1\left(b^{|s|} - 1\right)\mathrm{sgn}(s) - k_2|s|^a \mathrm{sgn}(s), \tag{16}$$

where $0 < a < 1$, $k_1 > 0$, $k_2 > 0$, and $b = 1 + k_2/k_1$. When the system state is far away from the sliding surface, the change rate of the first term in (16) is larger than that of the power function. It speeds up the reaching rate in the case $|s| > 1$. When the system state is near to the sliding surface, the second item in (16) can make the system approach the sliding surface with higher speed.

Finally, the proposed ISMRL-CNF scheme for system (3) is expressed as

$$\begin{aligned} u &= u_{\mathrm{CNF}} + u_{is} \\ &= Fx + Gr + \rho(y,r)B^T P(x - x_e) - k_1\left(b^{|s|} - 1\right)\mathrm{sgn}(s) - k_2|s|^a \mathrm{sgn}(s). \end{aligned} \tag{17}$$

Remark 1. In order to ensure the closed-loop system has a fast rise time, F is chosen such that the closed-loop poles of $C(sI - A + \mathrm{BF})^{-1}$ have a dominant pair with a small ration. F can be designed by using H_∞ optimization approach. In order to reduce the overshoot, $\rho(y,r)$ is selected to gradually change the damping ratio of the closed-loop system. To obtain the control parameters F, m, $\overline{\beta}$, and W properly, we have

$$\min_{F,m,\overline{\beta},W} = \int_0^\infty t|y - r|dt. \tag{18}$$

The integrated time and absolute error (ITAE) is utilized as the performance criteria, and the minimization problem (18) is solved by the particle swarm optimization (PSO) algorithm.

3.1. Demonstration of System Stability. Taking the derivative of the sliding surface (15) along the trajectories of system yields

$$\begin{aligned} \dot{s} &= B^+\left(\dot{x} - \left(Ax + B\left(\mathrm{sat}(u) - u_{is}\right)\right)\right) \\ &= B^+\left(Ax + \mathrm{Bsat}(u) + B\,d - \left(Ax + B\left(\mathrm{sat}(u) - u_{is}\right)\right)\right) \\ &= B^+\left(Bu_{is} + B\,d\right) \\ &= -k_1\left(b^{|s|} - 1\right)\mathrm{sgn}(s) - k_2|s|^a \mathrm{sgn}(s) + d. \end{aligned} \tag{19}$$

Defining a Lyapunov function $V_1 = 1/2s^2$ and taking the derivative of V_1 [44],

$$\begin{aligned} \dot{V}_1 &= s\dot{s} = s\left(-k_1\left(b^{|s|} - 1\right)\mathrm{sgn}(s) - k_2|s|^a \mathrm{sgn}(s) + d\right) \\ &= -k_1|s|\left(b^{|s|} - 1\right) - k_2|s|^{a+1} + s\,d \leq -k_1|s|\left(b^{|s|} - 1\right) - k_2|s|^{a+1} + |s||d| \leq -k_2|s|^{a+1} - \left(k_1\left(b^{|s|} - 1\right) - d_{\max}\right)|s|, \end{aligned} \tag{20}$$

where $|d| \leq d_{\max}$. It can be noted that when $k_1(b^{|s|} - 1) - d_{\max} \geq 0$ such that

$$|s| \geq \log_b\left(\frac{d_{\max} + k_1}{k_1}\right), \tag{21}$$

then $\dot{V}_1 \leq -k_2|s|^{a+1}$. Thus, the sliding mode variable s can converge to the finite-time convergence region $|s| \leq \log_b(d_{\max} + k_1/k_1)$ [44].

Take the control law into the system and let $\tilde{x} = x - x_e$, and we have

$$\dot{\tilde{x}} = (A + \mathrm{BF})\tilde{x} + B\psi, \tag{22}$$

where $\psi = \mathrm{sat}(F\tilde{x} + Hr + u_{\mathrm{NL}} + u_{\mathrm{is}}) - F\tilde{x} - Hr + d$.

Define a Lyapunov function:

$$V_2 = \tilde{x}^T P\tilde{x}. \tag{23}$$

Taking the derivative of V_2, we obtain

$$\begin{aligned} \dot{V}_2 &= \dot{\tilde{x}}^T P\tilde{x} + \tilde{x}^T P\dot{\tilde{x}} \\ &= \tilde{x}^T(A + \mathrm{BF})^T P\tilde{x} + \tilde{x}^T(A + \mathrm{BF})P\tilde{x} + 2\tilde{x}^T \mathrm{PB}\psi \\ &= -\tilde{x}^T W\tilde{x} + 2\tilde{x}^T \mathrm{PB}\psi. \end{aligned} \tag{24}$$

Then, we have

$$\left|F\tilde{x} + Hr + u_{is}\right| \leq |F\tilde{x}| + |Hr| + \left|u_{is}\right| \leq u_{\max}, \tag{25}$$

When $|F\tilde{x} + Hr + u_{NL} + u_{is}| \leq u_{\max}$, then

$$\psi = F\tilde{x} + Hr + u_{\mathrm{NL}} + u_{\mathrm{is}} - F\tilde{x} - Hr + d, \tag{26}$$

where $\dot{s}$ would converge to zero in finite time; then, $u_{is} = -d$. Then, $\psi = u_{\mathrm{NL}} = \rho(y,r)B^T P\tilde{x}$. $\rho(y,r)$ is a nonpositive function. So, $\dot{V}_2 \leq -\tilde{x}^T W\tilde{x}$.

When $(F\tilde{x} + Hr + u_{\mathrm{NL}} + u_{\mathrm{is}}) > u_{\max}$, then

$$\begin{aligned} u_{\mathrm{NL}} &< u_{\max} - \left(F\tilde{x} + Hr + u_{\mathrm{is}}\right) < 0, \\ \psi &= u_{\max} - (F\tilde{x} + Hr) + d \\ &= u_{\max} - \left(F\tilde{x} + Hr + u_{is}\right) \geq 0, \end{aligned} \tag{27}$$

where $\rho(y,r)$ is a nonpositive function. So, it implies that $\tilde{x}^T \mathrm{PB} \leq 0$. Then, $\dot{V}_2 \leq -\tilde{x}^T W\tilde{x}$.

When $(F\tilde{x} + Hr + u_{\mathrm{NL}} + u_{\mathrm{is}}) < -u_{\max}$, then

$$\begin{aligned} u_{\mathrm{NL}} &\leq -u_{\max} - F\tilde{x} - Hr - u_{\mathrm{is}} \leq 0, \\ \psi &= -u_{\max} - (F\tilde{x} + Hr) + d \\ &= -u_{\max} - \left(F\tilde{x} + Hr + u_{\mathrm{is}}\right) \leq 0, \end{aligned} \tag{28}$$

where $\rho(y,r)$ is a nonpositive function. So, it implies that $\tilde{x}^T \mathrm{PB} \leq 0$. Thus, $\dot{V}_2 \leq -\tilde{x}^T W\tilde{x}$. Therefore, we can summarize that $\dot{V}_2 \leq -\tilde{x}^T W\tilde{x} < 0$.

4. Simulation Results

In this section, various simulations are conducted to test the performance of the proposed strategy. For simplicity, system (2) is consider as linear systems with disturbances:

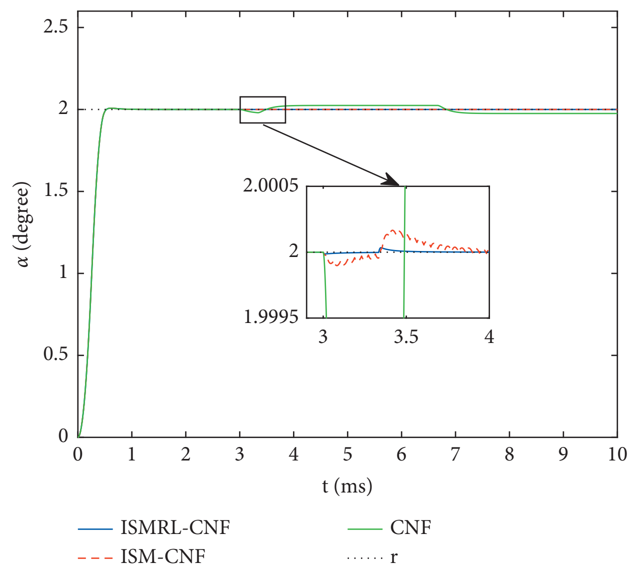

FIGURE 2: Comparison of angular α responses.

$$\begin{bmatrix} \dot{x}_1 \\ \dot{x}_2 \end{bmatrix} = \begin{bmatrix} 0 & 1 \\ -0.2251 & -0.16 \end{bmatrix} \begin{bmatrix} x_1 \\ x_2 \end{bmatrix} + \begin{bmatrix} 0 \\ 3.0827 \end{bmatrix} (\mathrm{sat}(u_\alpha) + d_\alpha), \quad y_1 = \begin{bmatrix} 1 & 0 \end{bmatrix} \begin{bmatrix} x_1 \\ x_2 \end{bmatrix}, \tag{29}$$

$$\begin{bmatrix} \dot{x}_3 \\ \dot{x}_4 \end{bmatrix} = \begin{bmatrix} 0 & 1 \\ -1 & -0.15 \end{bmatrix} \begin{bmatrix} x_3 \\ x_4 \end{bmatrix} + \begin{bmatrix} 0 \\ 1.7894 \end{bmatrix} (\mathrm{sat}(u_\beta) + d_\beta), \quad y_2 = \begin{bmatrix} 1 & 0 \end{bmatrix} \begin{bmatrix} x_3 \\ x_4 \end{bmatrix}, \tag{30}$$

where $u_\alpha = 10^6 T_\alpha$ and $u_\beta = 10^7 T_\beta$. The maximum inputs are $u_{\alpha\max} = u_{\beta\max} = 10$. The control objective is to force the scan angle α or β and follow the reference trajectory r precisely with fast response in presence of disturbances.

The parameters of CNF for system (29) are tuned by PSO as $F_\alpha = [-40.3457 \;\; -5.6301]$, $m_\alpha = 62.9236$, $\overline{\beta}_\alpha = 49.4610$, and $\theta_\alpha = -0.1296$. Then, $G_\alpha = 40.4187$, $W_\alpha = \begin{bmatrix} 0.7420 & 0 \\ 0 & 0.7420 \end{bmatrix}$, and $P_\alpha = \begin{bmatrix} 2.7124 & 0.0030 \\ 0.0030 & 0.0214 \end{bmatrix}$. The parameters of ISMRL are chosen as $k_{1\alpha} = 1$, $k_{2\alpha} = 1.6$, and $a_\alpha = 0.05$. The parameters of CNF for system (30) are tuned by PSO as $F_\beta = [-40.5216 \;\; -7.1381]$, $m_\beta = 4.5160$, $\overline{\beta}_\beta = 35.0126$, and $\theta_\beta = 0.4681$. Then, $G_\alpha = 41.0804 W_\beta = \begin{bmatrix} 2.9383 & 0 \\ 0 & 2.9383 \end{bmatrix}$ and $P_\beta = \begin{bmatrix} 8.7290 & 0.0200 \\ 0.0200 & 0.1152 \end{bmatrix}$. The parameters of ISMRL are chosen as $k_{1\beta} = 1.5$, $k_{2\beta} = 2.2$, and $a_\beta = 0.04$.

Figure 2 shows the MEMS micromirror along the x-axes tracking trajectories using the CNF, ISM-CNF, and proposed ISMRL-CNF controller, respectively. The target references for α are set as $r = 2$; the disturbance $d_\alpha = -\mathrm{sgn}(\sin(0.3\pi t))$ is introduced when $t \geq 3\,ms$. It can be noted that the proposed controller has better performance in comparison with the two other controller such as CNF and ISM-CNF. The actuation motion trajectory of the MEMS micromirror under the proposed ISMRL-CNF controller is consistent with the desired trajectory in presence of the disturbance. The closed-loop system has good transient performance such as very small overshoot and fast response. The control inputs of CNF, ISM-CNF, and ISMRL-CNF are shown in Figure 3; compared with ISM-CNF, the chattering problem is eliminated by using the proposed ISMRL-CNF.

Figure 4 shows the MEMS micromirror along the y-axes tracking trajectories using the CNF, ISM-CNF, and proposed ISMRL-CNF controller, respectively. The target references for β are set as $r = 2.2$ and the disturbance $d_\beta = -1.5\mathrm{sgn}(\sin(\pi t))$ is introduced when $t \geq 3.5\,ms$. The results demonstrate that the CNF controller exhibits worst performance due to the disturbances. Compare with ISM-CNF, the proposed ISMRL-CNF controller can obtain a faster and more efficient performance in presence of the disturbances. The control inputs of CNF, ISM-CNF, and proposed controller

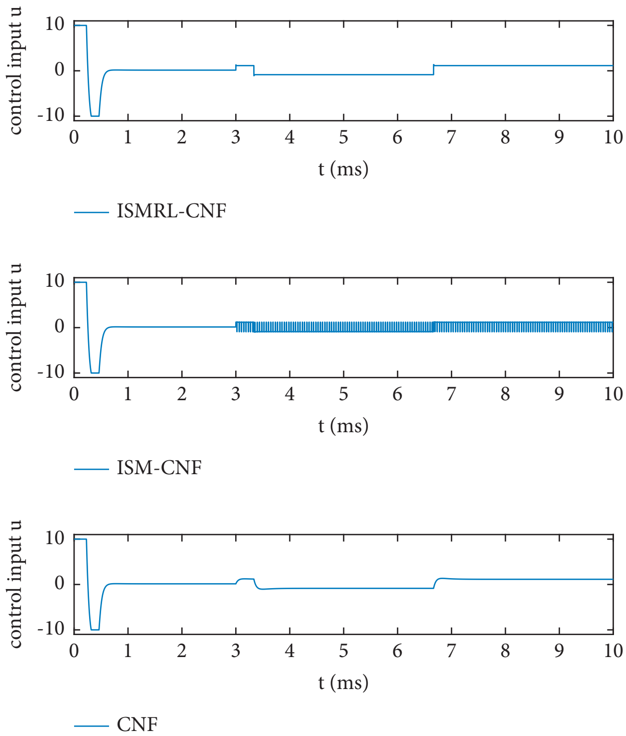

Figure 3: Control input u_α.

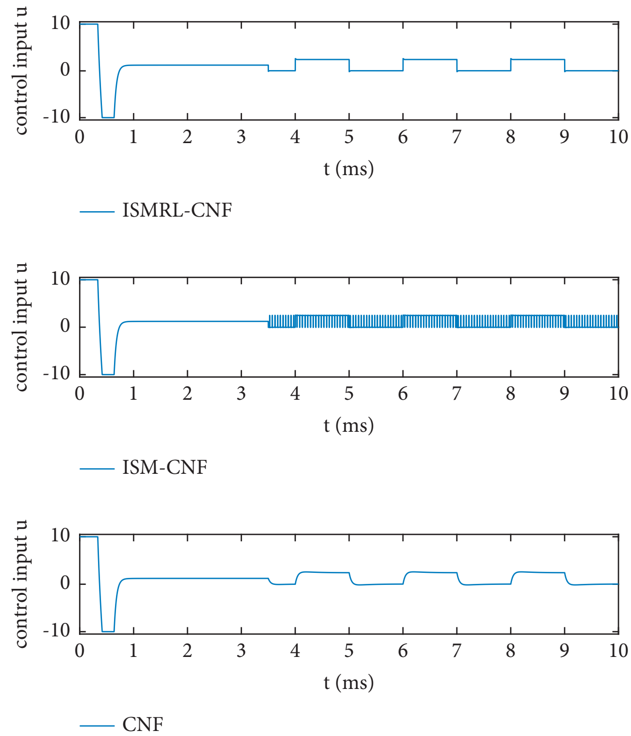

Figure 5: Control input u_β.

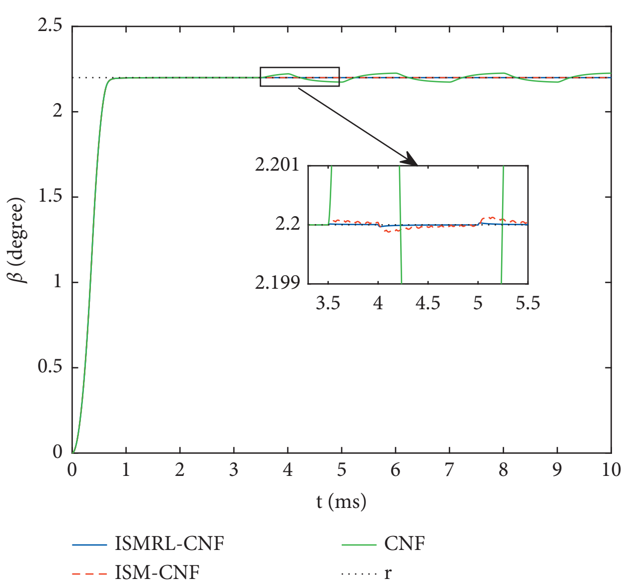

Figure 4: Comparison of angular β responses.

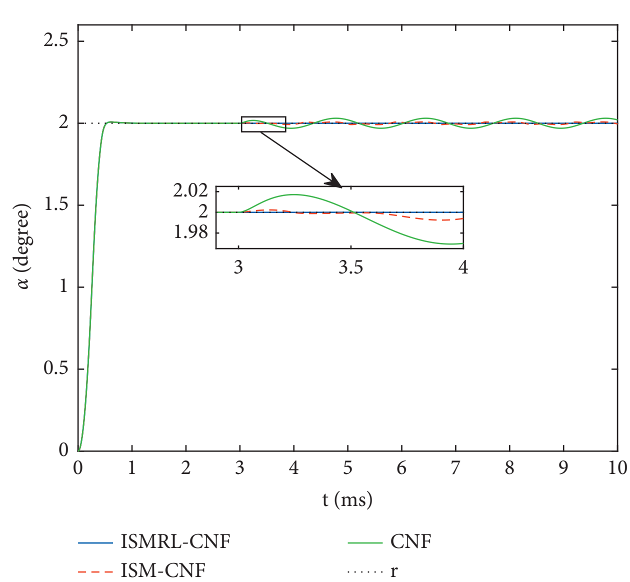

Figure 6: Comparison of angular α responses under disturbance $d = -1.5\sin(1.2\pi t)$.

are shown in Figure 5. It can be noted that the control input of ISMRL-CNF is more smoother than ISM-CNF.

To further verify the antidisturbances of the proposed controller, the time-varying disturbance is introduced.

The comparison of angular α responses using CNF, ISM-CNF, and proposed ISMRL-CNF controller under disturbance $d = -1.5\sin(1.2\pi t)$ is shown in Figure 6. It can be seen that the traditional CNF controller is not able to suppress the time-varying disturbance. Compared with ISM-CNF, the proposed ISMRL-CNF controller ensures the system has better response in presence of disturbance. The comparison of angular β responses using CNF, ISM-CNF, and proposed ISMRL-CNF controller under disturbance $d = -1.4\cos(1.3\pi t)$ is shown in Figure 7. The results demonstrate that the proposed controller ensures the system has better performance in presence of time-varying disturbance.

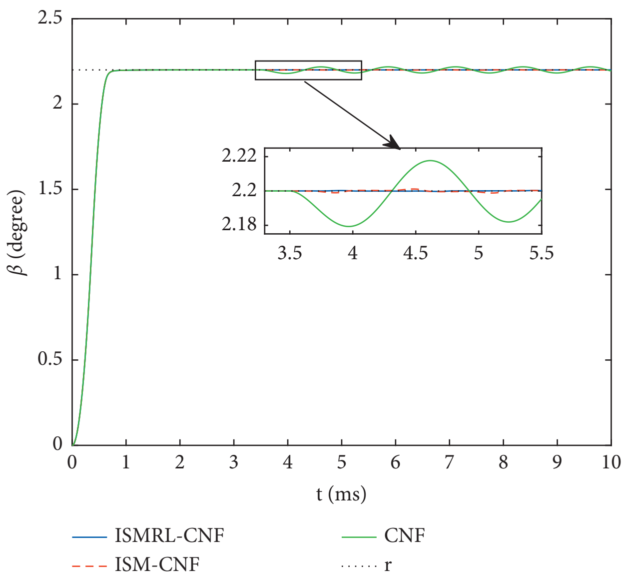

FIGURE 7: Comparison of angular β responses under disturbance $d = -1.4\cos(1.3\pi t)$.

5. Conclusions

In this study, the precise tracking problem for electrostatic micromirror systems with disturbances and input saturation is investigated. Inspired by the composite nonlinear feedback (CNF)'s improvement of the transient performance and the sliding mode control's enhancement of the robustness, a novel integral sliding mode with reaching law (ISMRL)-based composite nonlinear feedback (CNF) controller is proposed. Then, the stability of the closed-loop system is guaranteed based on Lyapunov theorem. Numerical simulations verify the effectiveness of the proposed scheme. It is shown that the closed-loop system with the proposed scheme has precise positioning and improved transient performance even in presence of time-varying disturbances. It should be noted that the proposed controller needs the accurate model knowledge; as a result, more inclusive methods about the model uncertainty and model inaccuracy, combined with faster convergence rate and smaller chattering, will be inquired in future work.

Data Availability

All data, models, or code that support the findings of this study are available from the corresponding author upon reasonable request.

Conflicts of Interest

The authors declare that they have no conflicts of interest.

Acknowledgments

This work was supported by National Science Foundation of China, under Grants 61603093 and 61703142.

References

[1] D. Wang, C. Watkins, and H. Xie, "MEMS mirrors for LiDAR: a review," *Micromachines*, vol. 11, no. 5, pp. 456–480, 2020.
[2] M. Saif, B. Ebrahimi, and M. Vali, "A second order sliding mode strategy for fault detection and fault-tolerant-control of a MEMS optical switch," *Mechatronics*, vol. 22, no. 6, pp. 696–705, 2012.
[3] Y. Lin, L. Keeler, and G. Ethan, "Progress of mems scanning micromirrors for optical bioimaging," *Micromachines*, vol. 6, 2015.
[4] A. D. Yalcinkaya, H. Urey, D. Brown, T. Montague, and R. Sprague, "Two-Axis electromagnetic microscanner for high resolution displays," *Journal of Microelectromechanical Systems*, vol. 15, no. 4, pp. 786–794, 2006.
[5] Y. Bai, J. T. W. Yeow, and B. C. Wilson, "A characteristic study of micromirror with sidewall electrodes," *International Journal of Optomechatronics*, vol. 1, no. 3, pp. 231–258, 2007.
[6] P. Zuo, G. Li, W. Xie, and J. T. W. Yeow, "Angle tracking of MEMS hard-magnetic micromirror by PID control," in *Proceedings of the 2015 34th Chinese Control Conference (CCC)*, pp. 593–597, Hangzhou, China, July 2015.
[7] C. G. Agudelo, M. Packirisamy, G. Guchuan Zhu, and L. Saydy, "Nonlinear control of an electrostatic micromirror beyond pull-in with experimental validation," *Journal of Microelectromechanical Systems*, vol. 18, no. 4, pp. 914–923, 2009.
[8] H. Chen, M. Li, Y. Zhang et al., "H_∞robust control of a large-piston MEMS micromirror for compact fourier transform spectrometer systems," *IEEE Sensors Journal*, vol. 18, no. 4, 2018.
[9] H. Chen, Z. Sun, W. Sun, and J. T. W. Yeow, "Twisting sliding mode control of an electrostatic MEMS micromirror for a laser scanning system," *IEEE/CAA Journal of Automatica Sinica*, vol. 6, no. 4, pp. 1060–1067, 2019.
[10] K. M Liao, Y. C. Wang, C. H. Yeh, and R. Chen, "Closed-loop adaptive control for electrostatically driven torsional micromirrors," *The Journal of Microlithography, Microfabrication, and Microsystems*, vol. 4, no. 4, 2005.
[11] Z. Lin, M. Pachter, and S. Banda, "Toward improvement of tracking performance nonlinear feedback for linear systems," *International Journal of Control*, vol. 70, no. 1, pp. 1–11, 1998.
[12] B. M. Chen, T. H. Lee, K. Kemao Peng, and V. Venkataramanan, "Composite nonlinear feedback control for linear systems with input saturation: theory and an application," *IEEE Transactions on Automatic Control*, vol. 48, no. 3, pp. 427–439, 2003.
[13] W. Lan, B. M. Chen, and Y. He, "On improvement of transient performance in tracking control for a class of nonlinear systems with input saturation," *Systems & Control Letters*, vol. 55, no. 2, pp. 132–138, 2006.
[14] S. Mobayen and F. Tchier, "Composite nonlinear feedback control technique for master/slave synchronization of nonlinear systems," *Nonlinear Dynamics*, vol. 87, no. 3, pp. 1731–1747, 2016.
[15] S. Singh, S. Purwar, and A. Kulkarni, "Two term composite nonlinear feedback controller design for nonlinear time-delay systems," *Transactions of the Institute of Measurement and Control*, vol. 40, no. 12, pp. 3424–3432, 2017.
[16] T. Lu and W. Lan, "Composite nonlinear feedback control for strict-feedback nonlinear systems with input saturation," *International Journal of Control*, vol. 92, no. 9, pp. 2170–2177, 2019.

[17] T. Yang, N. Sun, and Y. Fang, "Neuroadaptive control for complicated underactuated systems with simultaneous output and velocity constraints exerted on both actuated and unactuated states," *IEEE Transactions on Neural Networks and Learning Systems*, 2021, in press.

[18] E. Jafari and T. Binazadeh, "Observer-based improved composite nonlinear feedback control for output tracking of time-varying references in descriptor systems with actuator saturation," *ISA Transactions*, vol. 91, pp. 1–10, 2019.

[19] W. Weiyao Lan, C. K. Chin Kwan Thum, and B. M. Chen, "A hard-disk-drive servo system design using composite non-linear-feedback control with optimal nonlinear gain tuning methods," *IEEE Transactions on Industrial Electronics*, vol. 57, no. 5, pp. 1735–1745, 2010.

[20] H. Namdari, F. Allahverdizadeh, and A. Sharifi, "Robust composite nonlinear feedback control for spacecraft rendezvous systems under parameter uncertainty, external disturbance, and input saturation," *Proceedings of the Institution of Mechanical Engineers - Part G: Journal of Aerospace Engineering*, vol. 234, no. 2, pp. 143–155, 2018.

[21] Z. Hou and I. Fantoni, "Interactive leader-follower consensus of multiple quadrotors based on composite nonlinear feedback control," *IEEE Transactions on Control Systems Technology*, vol. 26, no. 5, pp. 1732–1743, 2018.

[22] Y. Jiang, K. Lu, C. Gong, and H. Liang, "Robust composite nonlinear feedback control for uncertain robot manipulators," *International Journal of Advanced Robotic Systems*, vol. 17, no. 2, pp. 1–9, 2020.

[23] Y. Chen, C. Hu, and J. Wang, "Motion planning with velocity prediction and composite nonlinear feedback tracking control for lane-change strategy of autonomous vehicles," *IEEE Transactions on Intelligent Vehicles*, vol. 5, no. 1, pp. 63–74, 2020.

[24] F. Castanos and L. Fridman, "Analysis and design of integral sliding manifolds for systems with unmatched perturbations," *IEEE Transactions on Automatic Control*, vol. 51, no. 5, pp. 853–858, 2006.

[25] G. Sun, Z. Ma, and J. Yu, "Discrete-time fractional order terminal sliding mode tracking control for linear motor," *IEEE Transactions on Industrial Electronics*, vol. 65, no. 4, pp. 3386–3394, 2018.

[26] H. Wang, L. Hua, Y. Guo, and C. Lu, "Control of Z-axis MEMS gyroscope using adaptive fractional order dynamic sliding mode approach," *IEEE Access*, vol. 7, pp. 133008–133016, 2019.

[27] B. Bandyopadhyay, D. Fulwani, and Y. J. Park, "A robust algorithm against actuator saturation using integral sliding mode and composite nonlinear feedback," in *Proceedings of the 17th IFAC World Congress*, pp. 14174–14179, Seoul, Korea, July 2008.

[28] J. Tan, W. Sun, and J. T. W. Yeow, "An enhanced robust control algorithm based on CNF and ISM for the MEMS micromirror against input saturation and disturbance," *Micromachines*, vol. 8, no. 8, 2017.

[29] S. Mobayen, V. J. Majd, and M. Sojoodi, "An LMI-based composite nonlinear feedback terminal sliding-mode controller design for disturbed MIMO systems," *Mathematics and Computers in Simulation*, vol. 85, pp. 1–10, 2012.

[30] S. Mobayen, M. H. Asemani, and V. J. Majd, "Transient performance improvement using composite nonlinear feedback and integral sliding surface for matched and unmatched uncertain MIMO linear systems," in *Proceedings of the 3rd ICCIA*, pp. 83–88, Tehran, Iran, December 2013.

[31] S. Mobayen, "Design of CNF-based nonlinear integral sliding surface for matched uncertain linear systems with multiple state-delays," *Nonlinear Dynamics*, vol. 77, no. 3, pp. 1047–1054, 2014.

[32] V. J. Majd and S. Mobayen, "An ISM-based CNF tracking controller design for uncertain MIMO linear systems with multiple time-delays and external disturbances," *Nonlinear Dynamics*, vol. 80, no. 1-2, pp. 591–613, 2015.

[33] C. Hu, R. Wang, and F. Yan, "Integral sliding mode-based composite nonlinear feedback control for path following of four-wheel independently actuated autonomous vehicles," *IEEE Transactions on Transportation Electrification*, vol. 2, no. 2, pp. 221–230, 2016.

[34] C. Hu, R. Wang, F. Yan, M. Chadli, Y. Huang, and H. Wang, "Robust path-following control for a fully actuated marine surface vessel with composite nonlinear feedback," *Transactions of the Institute of Measurement and Control*, vol. 40, no. 12, pp. 3477–3488, 2017.

[35] S. Mobayen and F. Tchier, "Composite nonlinear feedback integral sliding mode tracker design for uncertain switched systems with input saturation," *Communications in Nonlinear Science and Numerical Simulation*, vol. 65, pp. 173–184, 2018.

[36] S. Mobayen, "Chaos synchronization of uncertain chaotic systems using composite nonlinear feedback based integral sliding mode control," *ISA Transactions*, vol. 77, pp. 100–111, 2018.

[37] P. S. Babu and B. Bandyopadhyay, "Integral sliding mode based composite nonlinear feedback control for descriptor systems," *IFAC-Papers On Line*, vol. 51, no. 1, pp. 598–603, 2018.

[38] P. S. Babu, B. Bandyopadhyay, and M. Thomas, "Robust composite non-linear feedback control for descriptor systems with general reference tracking," in *Proceedings of the IECON 2018-44th Annual Conference of the IEEE Industrial Electronics Society*, pp. 2434–2439, Washington, DC, USA, October 2018.

[39] T. Yang, N. Sun, and Y. Fang, "Adaptive fuzzy control for a class of MIMO underactuated systems with plant uncertainties and actuator deadzones: design and experiments," *IEEE Transactions on Cybernetics*, vol. 99, pp. 1–14, 2021.

[40] H. Chen, B. Guan, Y. Zhou, W. Sun, and J. T. W. Yeow, "Optimal second order integral sliding mode based composite nonlinear feedback approach for an electrostatic micromirror," *IEEE Access*, vol. 8, pp. 145960–145967, 2020.

[41] A. Pati and R. Negi, "Super-twisting algorithm-based integral sliding mode control with composite nonlinear feedback control for magnetic levitation system," *International Journal of Automation and Control*, vol. 13, no. 6, pp. 717–734, 2019.

[42] W. Weibing Gao and J. C. Hung, "Variable structure control of nonlinear systems: a new approach," *IEEE Transactions on Industrial Electronics*, vol. 40, no. 1, pp. 45–55, 1993.

[43] H. Ma, J. Wu, and Z. Xiong, "A novel exponential reaching law of discrete-time sliding-mode control," *IEEE Transactions on Industrial Electronics*, vol. 64, no. 5, pp. 3840–3850, 2017.

[44] C. B. Xiu and P. H. Gao, "Global terminal sliding mode control with the quick reaching law and its application," *IEEE Access*, vol. 6, pp. 1–8, 2018.

[45] H. Pan, G. Zhang, H. Ouyang, and L. Mei, "A novel global fast terminal sliding mode control scheme for second-order systems," *IEEE Access*, vol. 8, pp. 22758–22769, 2020.